PHYSICAL REVIEW D **91,** 024007 (2015)

Geometrothermodynamics of black holes in Lovelock gravity with a nonlinear electrodynamics

S. H. Hendi[1,2,*] and R. Naderi[3,†]

[1]*Physics Department and Biruni Observatory, College of Sciences, Shiraz University, Shiraz 71454, Iran*
[2]*Research Institute for Astrophysics and Astronomy of Maragha (RIAAM), P.O. Box 55134-441 Maragha, Iran*
[3]*Department of Physics, Azarbaijan Shahid Madani University, Tabriz 53714-161, Iran*
(Received 28 October 2014; published 5 January 2015)

The objective of the present paper is to analyze the phase transition of asymptotically anti–de Sitter (AdS) black-hole solutions in Lovelock gravity in the presence of nonlinear electrodynamics. First, we present the asymptotically AdS black-hole solutions for two classes of the Born-Infeld type of nonlinear electrodynamics coupled (separately) with Einstein, Gauss-Bonnet, and third-order Lovelock gravity. Then, in order to discuss the phase transition, we calculate both the heat capacity and the Ricci scalar of the thermodynamical line element. We present a comparison between the singular points of the Ricci scalar using the geometrothermodynamics method and the corresponding vanishing points of the heat capacity in the canonical ensemble. In addition, we discuss the effects of both Lovelock and nonlinear electrodynamics on the phase transition points.

DOI: 10.1103/PhysRevD.91.024007 PACS numbers: 04.40.Nr, 04.20.Jb, 04.70.Bw, 04.70.Dy

I. INTRODUCTION

One of the more interesting tools for studying a thermodynamical system are phase transitions. In order to investigate phase transitions, one may use the microcanonical, canonical, and/or grand canonical ensembles.

On the other hand, phase transitions of a thermodynamical systems may be investigated by using the concept of geometry in thermodynamics—the so-called geometrothermodynamics (GTD). In this method one may define a thermodynamical line element, and curvature can be interpreted as a system interaction. One can study the phase transitions by obtaining the curvature singularities of the thermodynamical metric. Although the equivalence of these two methods—i.e., the roots of the heat capacity in the canonical ensemble (computed by using standard black-hole thermodynamics) and the curvature singularities of the thermodynamical metric (calculated using the GTD approach)—has been checked for asymptotically anti–de Sitter (AdS) black holes [1], it is not in general on firm ground [2] and so an investigation of the validity of such an equivalence may be worthwhile, especially in cases with nonlinear electrodynamics (NLED) sources.

At first, Weinhold defined the second derivatives of the internal energy with respect to entropy and other extensive quantities (such as the electric charge) of a thermodynamical system to introduce a Riemannian metric [3,4],

$$g^W = \frac{\partial^2 M}{\partial X^i \partial X^j} dX^i dX^j, \qquad X^i = X^i(S,Q). \tag{1}$$

Then, Ruppeiner introduced another metric, in which the Riemannian metric was defined as the negative Hessian of the entropy with respect to the internal energy and other extensive quantities of a thermodynamical system [5,6],

$$g^R = \frac{\partial^2 S}{\partial Y^i \partial Y^j} dY^i dY^j, \qquad Y^i = Y^i(M,Q). \tag{2}$$

It was shown that both the Ruppeiner and Weinhold metrics are conformally related to each other, where temperature is the conformal factor [7]. Recently, it was shown that the phase transition points of the heat capacity do not match those in the Weinhold and Ruppeiner metrics. Quevedo has established a new Legendre-invariant thermodynamical line element to overcome this problem [1,8–13]. Although there is more than one Legendre-invariant metric, in this paper we use the simplest Legendre-invariant generalization of the Weinhold metric, g^W, which can be written as

$$g = Mg^W = M\frac{\partial^2 M}{\partial X^a \partial X^b} dX^a dX^b, \tag{3}$$

where $X^a = \{S, Q\}$ and its Legendre-invariant metric can be written in terms of the Ruppeiner metric, g^R, as

$$g = MTg^R = -\frac{M}{(\frac{\partial S}{\partial M})}\frac{\partial^2 S}{\partial Y^a \partial Y^b} dY^a dY^b, \tag{4}$$

where $Y^a = \{M, Q\}$.

In this paper, we follow the Quevedo method to study GTD in Einstein, Gauss-Bonnet (GB), and third-order

* hendi@shirazu.ac.ir
† r.naderi@azaruniv.edu

Lovelock (TOL) gravities [14]. In addition, we consider the recently proposed Born-Infeld (BI)-type models of NLED as a source [15] (motivations for the Lovelock and BI-type models can be found in Refs. [16–19]). We should note that although one can study the constant-curvature spacetimes with positive, zero, or negative values for Λ, the case of a negative cosmological constant is of interest for studies of the AdS/CFT correspondence [20]. Besides, the Hawking-Page phase transition can be interpreted using the AdS/CFT correspondence. So, hereafter we are interested only in asymptotically AdS solutions.

The plan of the paper is as follows. In Sec. II, we give a brief discussion of the asymptotically AdS black-hole solutions of Einstein, GB, and TOL gravities in the presence of NLED. Section III is devoted to the calculation of conserved and thermodynamic quantities and a check of the first law of thermodynamics. Then, we discuss the thermal stability of the solutions by calculating the heat capacity. We use the concept of geometry in thermodynamics to study the phase transition. We also compare GTD results with the canonical ensemble stability criterion. Finally, we end with some conclusions.

II. ASYMPTOTICALLY AdS BLACK-HOLE SOLUTIONS OF LOVELOCK GRAVITY WITH BI-TYPE NLED

The Lagrangian of Lovelock gravity coupled with a NLED source is written as [14]

$$\pounds = \mathcal{L}_{\mathrm{Lovelock}} + \mathcal{L}(\mathcal{F}), \tag{5}$$

$$\mathcal{L}_{\mathrm{Lovelock}} = \sum_{i=0} \alpha_i \mathcal{L}_i, \tag{6}$$

where α_i and $\mathcal{L}_i$ indicate the coefficients and Lagrangians of Lovelock gravity, respectively, and $\mathcal{L}(\mathcal{F})$ is the Lagrangian of NLED. In this paper, we regard Lovelock gravity up to the fourth term. More explicitly, $\mathcal{L}_0 = -2\Lambda$, in which Λ is the negative cosmological constant, $\mathcal{L}_1 = R$ denotes the Ricci scalar, $\mathcal{L}_2 = R_{\mu\nu\gamma\delta}R^{\mu\nu\gamma\delta} - 4R_{\mu\nu}R^{\mu\nu} + R^2$ is the Lagrangian of Gauss-Bonnet gravity, and the Lagrangian of third-order Lovelock gravity, $\mathcal{L}_3$, is

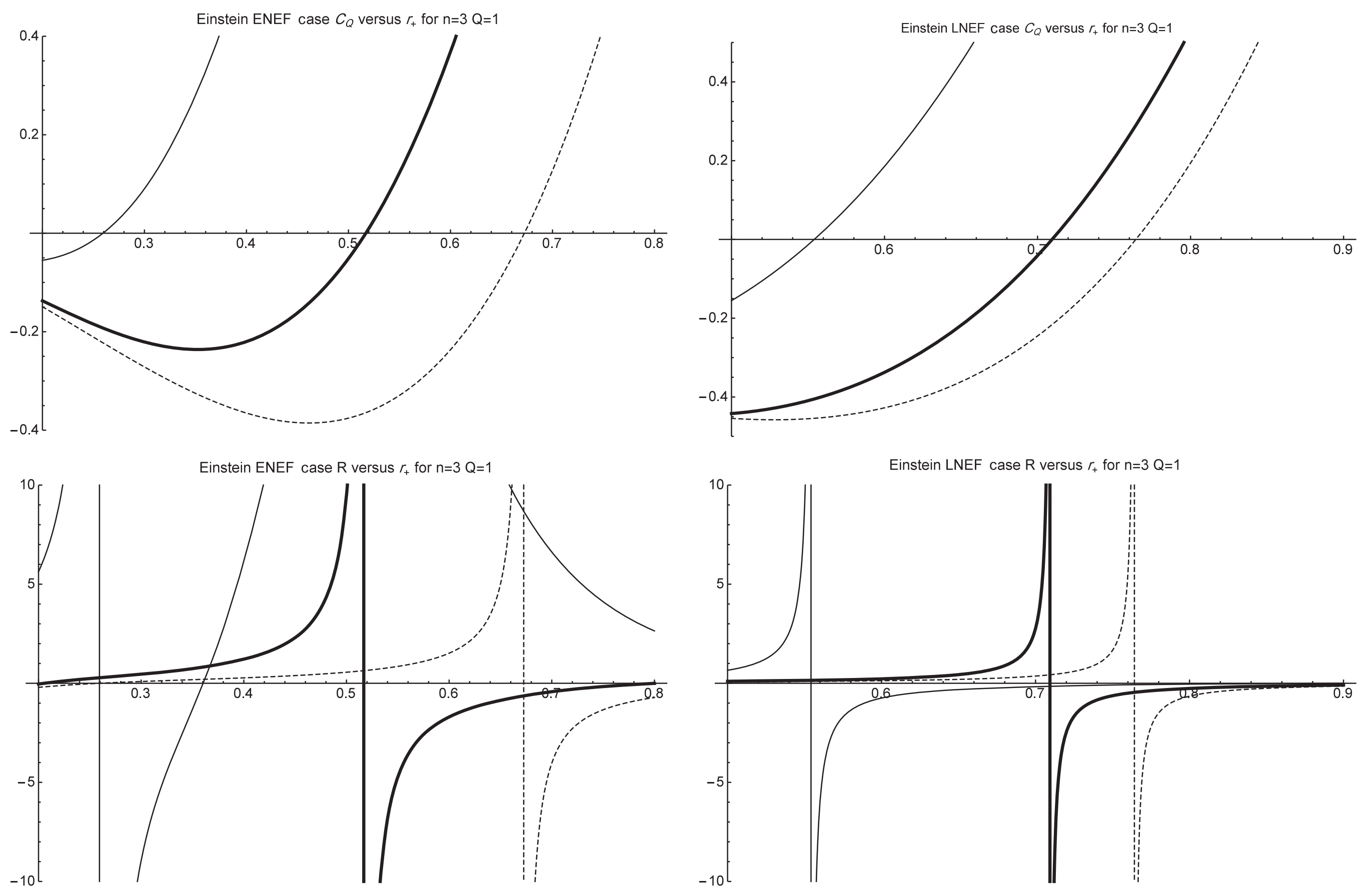

FIG. 1. Einstein case: ENEF (left) and LNEF (right) branches. The heat capacity (top) and geometric Ricci scalar (bottom) are shown versus r_+ for $n = 3$, $\Lambda = -1$, $Q = 1$, and $\beta = 0.5$ (solid line), $\beta = 1$ (bold line), and $\beta = 2$ (dashed line).

$$\mathcal{L}_3 = 2R^{\mu\nu\sigma\kappa}R_{\sigma\kappa\rho\tau}R^{\rho\tau}{}_{\mu\nu} + 8R^{\mu\nu}{}_{\sigma\rho}R^{\sigma\kappa}{}_{\nu\tau}R^{\rho\tau}{}_{\mu\kappa} + 24R^{\mu\nu\sigma\kappa}R_{\sigma\kappa\nu\rho}R^{\rho}{}_{\mu} + 3RR^{\mu\nu\sigma\kappa}R_{\sigma\kappa\mu\nu} + 24R^{\mu\nu\sigma\kappa}R_{\sigma\mu}R_{\kappa\nu} + 16R^{\mu\nu}R_{\nu\sigma}R^{\sigma}{}_{\mu} - 12RR^{\mu\nu}R_{\mu\nu} + R^3. \tag{7}$$

In order to consider an appropriate model of NLED, we take into account the recently proposed BI-type models of NLED which were introduced by Hendi (exponential form of nonlinear electromagnetic field or ENEF) [15] and Soleng (logarithmic form of nonlinear electromagnetic field or LNEF) [21] with the following explicit forms:

$$\mathcal{L}(\mathcal{F}) = \begin{cases} \beta^2(\exp(-\frac{\mathcal{F}}{\beta^2}) - 1), & \text{(ENEF)} \\ -8\beta^2 \ln(1 + \frac{\mathcal{F}}{8\beta^2}), & \text{(LNEF)} \end{cases} \tag{8}$$

where β denotes the nonlinearity parameter and the Maxwell invariant is $\mathcal{F} = F_{ab}F^{ab}$, in which $F_{ab} = \partial_a A_b - \partial_b A_a$ is the electromagnetic field tensor and A_a is the gauge potential. We should note that for large values of β, the Lagrangians of Eq. (8) reduce to the linear Maxwell Lagrangian.

Taking into account both gravitational (g^{ab}) and electromagnetic (A^a) fields, and using the Euler-Lagrange equation, the field equations of Lovelock gravity in the presence of NLED are described by [22]

$$\alpha_0 G^{(0)}_{\mu\nu} + \alpha_1 G^{(1)}_{\mu\nu} + \alpha_2 G^{(2)}_{\mu\nu} + \alpha_3 G^{(3)}_{\mu\nu} = \frac{1}{2} g_{\mu\nu}\mathcal{L}(\mathcal{F}) - 2F_{\mu\lambda}F^{\lambda}_{\nu}\mathcal{L}_{\mathcal{F}} \tag{9}$$

and

$$\partial_\mu(\sqrt{-g}\mathcal{L}_{\mathcal{F}}F^{\mu\nu}) = 0, \tag{10}$$

where $\alpha_0 = \alpha_1 = 1$, the arbitrary coefficients α_2 and α_3 are related to GB and TOL gravity, and

$$G^{(0)}_{\mu\nu} = -\frac{1}{2} g_{\mu\nu}\mathcal{L}_0, \tag{11}$$

$$G^{(1)}_{\mu\nu} = R_{\mu\nu} - \frac{1}{2} g_{\mu\nu}\mathcal{L}_1, \tag{12}$$

$$G^{(2)}_{\mu\nu} = 2(R_{\mu\sigma\kappa\tau}R_{\nu}{}^{\sigma\kappa\tau} - 2R_{\mu\rho\nu\sigma}R^{\rho\sigma} - 2R_{\mu\sigma}R^{\sigma}{}_{\nu} + RR_{\mu\nu}) - \frac{1}{2} g_{\mu\nu}\mathcal{L}_2, \tag{13}$$

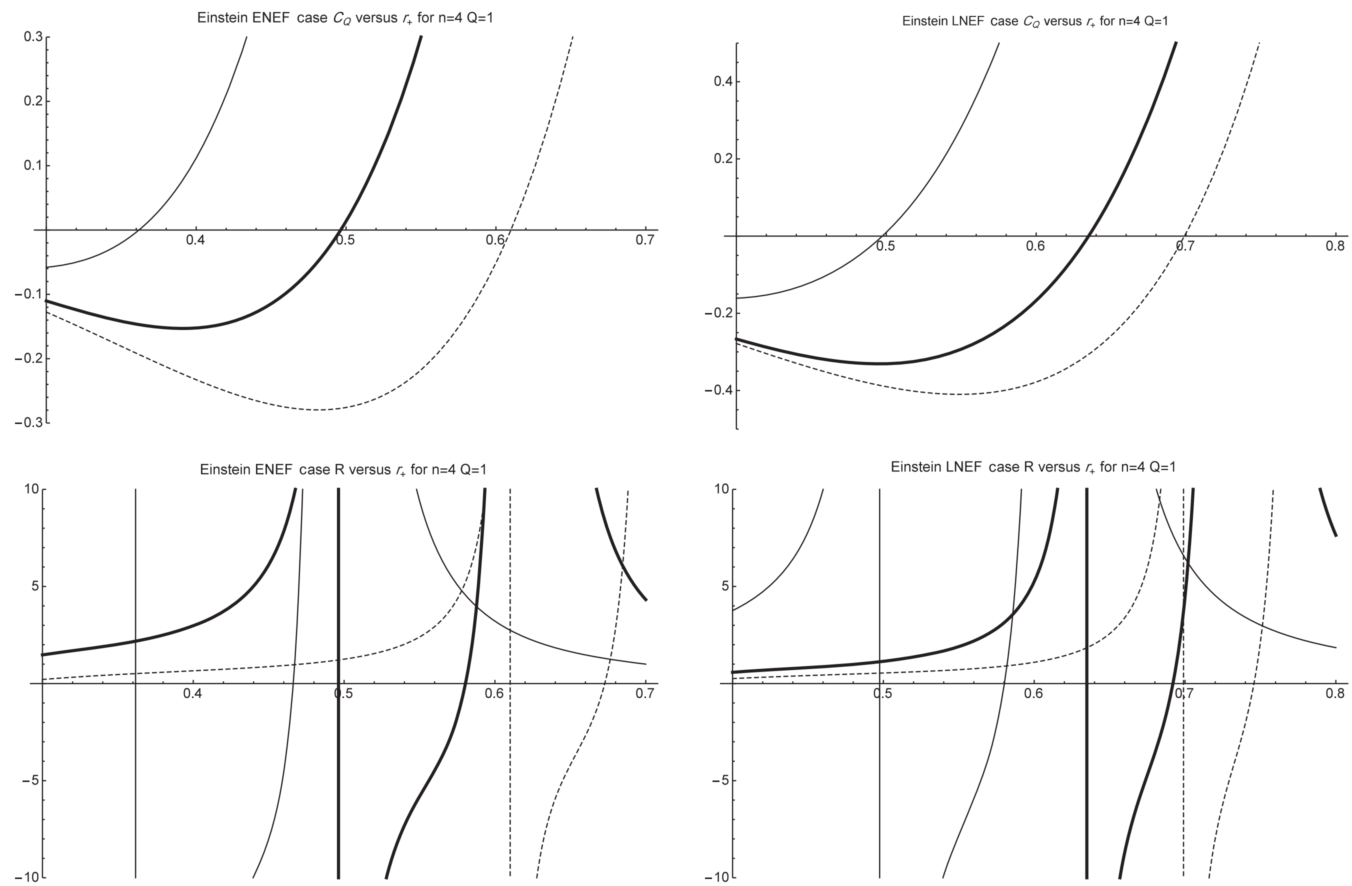

FIG. 2. Einstein case: ENEF (left) and LNEF (right) branches. The heat capacity (top) and geometric Ricci scalar (bottom) are shown versus r_+ for $n = 4$, $\Lambda = -1$, $Q = 1$, and $\beta = 0.5$ (solid line), $\beta = 1$ (bold line), and $\beta = 2$ (dashed line).

$$G^{(3)}_{\mu\nu} = -3(4R^{\tau\rho\sigma\kappa}R_{\sigma\kappa\lambda\rho}R^{\lambda}{}_{\nu\tau\mu} - 8R^{\tau\rho}{}_{\lambda\sigma}R^{\sigma\kappa}{}_{\tau\mu}R^{\lambda}{}_{\nu\rho\kappa} + 2R_{\nu}{}^{\tau\sigma\kappa}R_{\sigma\kappa\lambda\rho}R^{\lambda\rho}{}_{\tau\mu} - R^{\tau\rho\sigma\kappa}R_{\sigma\kappa\tau\rho}R_{\nu\mu} + 8R^{\tau}{}_{\nu\sigma\rho}R^{\sigma\kappa}{}_{\tau\mu}R^{\rho}{}_{\kappa} + 8R^{\sigma}{}_{\nu\tau\kappa}R^{\tau\rho}{}_{\sigma\mu}R^{\kappa}{}_{\rho}$$
$$+ 4R_{\nu}{}^{\tau\sigma\kappa}R_{\sigma\kappa\mu\rho}R^{\rho}{}_{\tau} - 4R_{\nu}{}^{\tau\sigma\kappa}R_{\sigma\kappa\tau\rho}R^{\rho}{}_{\mu} + 4R^{\tau\rho\sigma\kappa}R_{\sigma\kappa\tau\mu}R_{\nu\rho} + 2RR_{\nu}{}^{\kappa\tau\rho}R_{\tau\rho\kappa\mu} + 8R^{\tau}{}_{\nu\mu\rho}R^{\rho}{}_{\sigma}R^{\sigma}{}_{\tau} - 8R^{\sigma}{}_{\nu\tau\rho}R^{\tau}{}_{\sigma}R^{\rho}_{\mu}$$
$$- 8R^{\tau\rho}{}_{\sigma\mu}R^{\sigma}{}_{\tau}R_{\nu\rho} - 4RR^{\tau}{}_{\nu\mu\rho}R^{\rho}{}_{\tau} + 4R^{\tau\rho}R_{\rho\tau}R_{\nu\mu} - 8R^{\tau}{}_{\nu}R_{\tau\rho}R^{\rho}{}_{\mu} + 4RR_{\nu\rho}R^{\rho}{}_{\mu} - R^{2}R_{\nu\mu}) - \frac{1}{2}\mathcal{L}_{3}g_{\mu\nu}, \tag{14}$$

and $\mathcal{L}_{\mathcal{F}} = \frac{d\mathcal{L}(\mathcal{F})}{d\mathcal{F}}$.

Now, we should consider a suitable metric and study the effects of both the Lovelock and NLED terms. The $(n+1)$-dimensional line element of a spherically symmetric spacetime may be written as

$$ds^2 = -N(r)f(r)dt^2 + \frac{dr^2}{f(r)} + r^2\left(d\theta_1^2 + \sum_{i=2}^{n-1}\prod_{j=1}^{i-1}\sin^2\theta_j d\theta_i^2\right), \tag{15}$$

and hereafter we suppose that the volume of a $(n-1)$-dimensional, $t=$ const, and $r=$ const hypersurface is V_{n-1}. The nonzero components of the electromagnetic field tensor in arbitrary $(n+1)$ dimensions may be written as [18,19]

$$F_{tr} = -F_{rt} = \frac{q}{r^{n-1}} \times \begin{cases} \exp\left(-\frac{L_W}{2}\right), & \text{(ENEF)} \\ \frac{2}{1+\Gamma}, & \text{(LNEF)} \end{cases} \tag{16}$$

where

$$L_W = \mathrm{Lambert}W\left(\frac{4q^2}{\beta^2 r^{2n-2}}\right),$$

$$\Gamma = \sqrt{1 + \frac{q^2}{\beta^2 r^{2n-2}}},$$

and q is an integration constant related to the electric charge. The metric function of Einstein gravity that satisfies the gravitational field equation ($\alpha_2 = \alpha_3 = 0$) is [18,19]

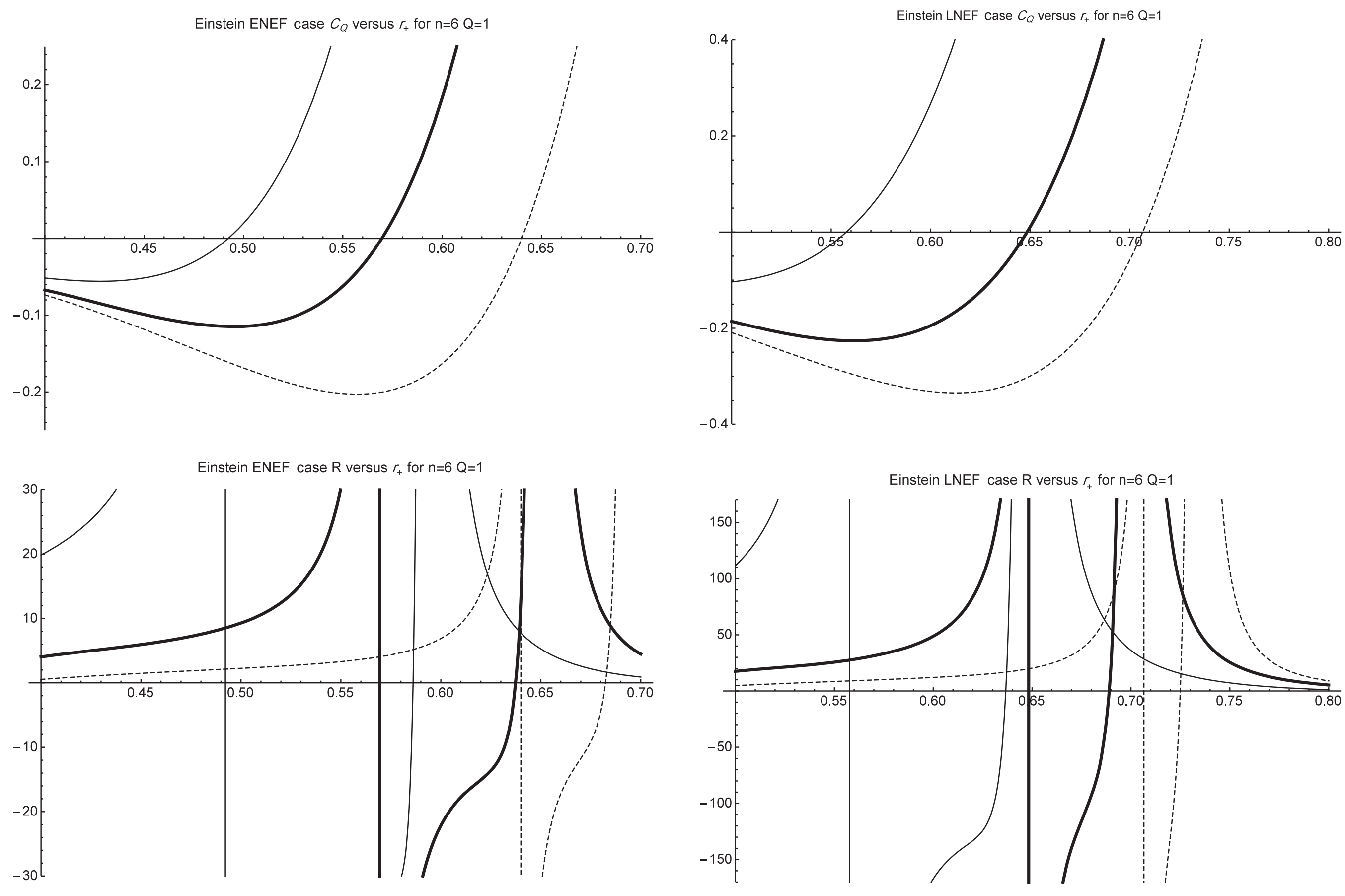

FIG. 3. Einstein case: ENEF (left) and LNEF (right) branches. The heat capacity (top) and geometric Ricci scalar (bottom) are shown versus r_+ for $n=6$, $\Lambda=-1$, $Q=1$, and $\beta=0.5$ (solid line), $\beta=1$ (bold line), and $\beta=2$ (dashed line).

$$f_E(r) = 1 - \frac{2\Lambda r^2}{n(n-1)} - \frac{m}{r^{n-2}} + \Sigma, \tag{17}$$

where

$$\Sigma = \begin{cases} -\frac{\beta^2 r^2}{n(n-1)} + \frac{2q\beta}{(n-1)r^{n-2}} \int \frac{1-L_W}{\sqrt{L_W}} dr, & \text{(ENEF)} \\ -\frac{16\beta^2 r^2}{n(n-1)} - \frac{8\beta^2 \ln(2)}{n(n-1)} + \frac{8}{(n-1)r^{n-2}} \int \frac{\frac{q^2}{\Gamma-1} - \beta^2 \ln\left(\frac{\beta^2 r^{2n-2}(\Gamma-1)}{q^2}\right)}{r^{n-1}} dr, & \text{(LNEF)} \end{cases} \tag{18}$$

and m is an integration constant related to the finite mass. Looking at last the term of Eq. (18), one may think that, for some specific limits, this term behaves like a mass term (proportional to r^{2-n}); however, this is not true. We should note that the only integration constant of the field equation was labeled with m in Eq. (17) and we cannot adjust q and β to obtain a constant value for the integration part of the last term in Eq. (18) for arbitrary r [18,19].

The metric function for GB gravity ($\alpha_2 \neq 0$, $\alpha_3 = 0$) can be written as [16]

$$f_{\rm GB}(r) = 1 + \frac{r^2}{2\alpha}\left(1 - \sqrt{\Psi_{\rm GB}}\right), \tag{19}$$

where

$$\Psi_{\rm GB} = 1 + \frac{8\alpha\Lambda}{n(n-1)} + \frac{4\alpha m}{r^n} + \frac{4\alpha\beta^2\Upsilon_n}{n(n-1)}, \tag{20}$$

$$\Upsilon_n = \begin{cases} 1 + \frac{2nq}{\beta r^n} \int \frac{L_W - 1}{\sqrt{L_W}} dr, & \text{(ENEF)} \\ \frac{8(n-1)}{n}\left[\frac{(2n-1)(\Gamma-1)}{n-1} - \frac{n\ln\left(\frac{1+\Gamma}{2}\right)}{n-1} + \frac{(n-1)(1-\Gamma^2)\mathcal{H}}{n-2}\right], & \text{(LNEF)} \end{cases} \tag{21}$$

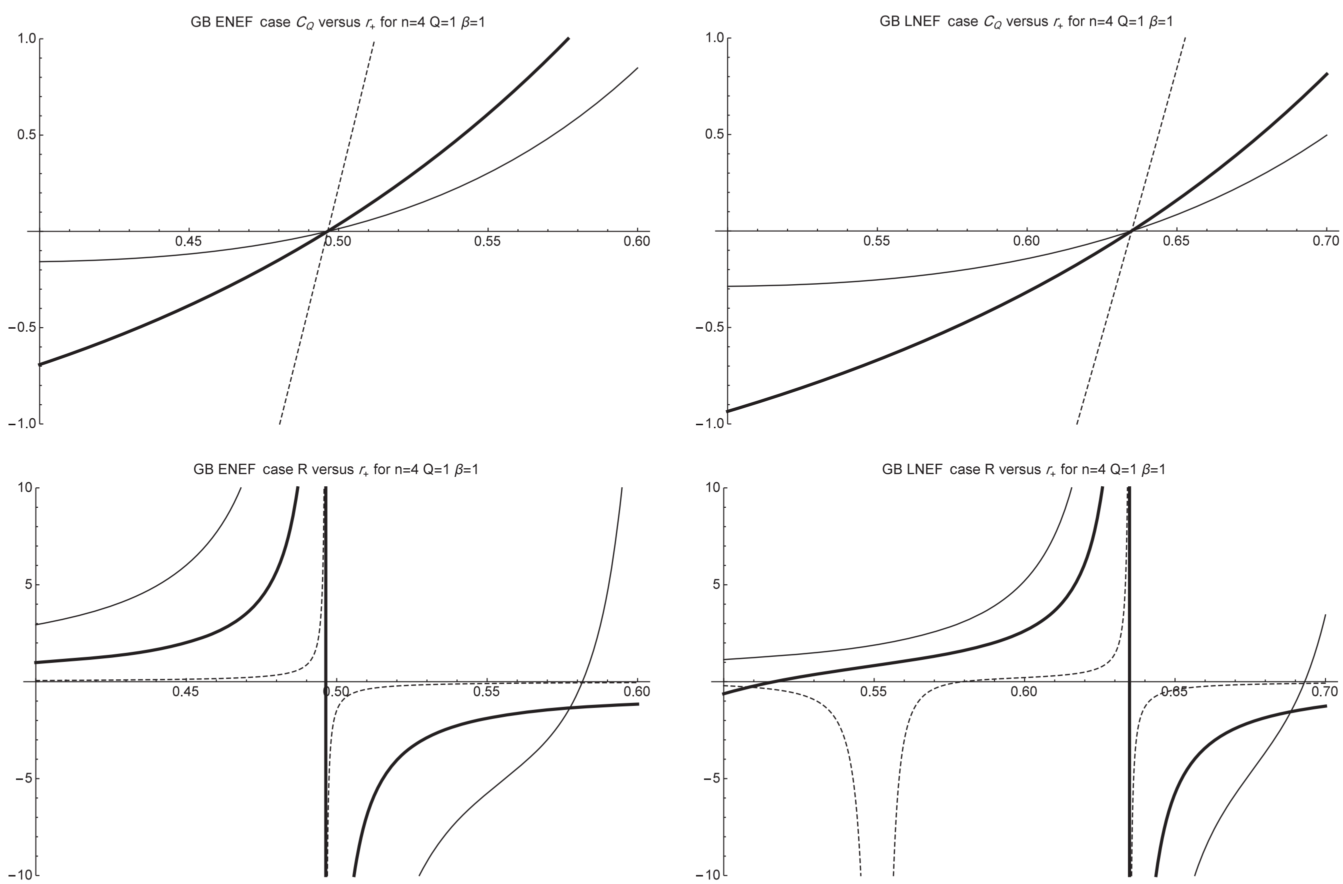

FIG. 4. GB case: ENEF (left) and LNEF (right) branches. The heat capacity (top) and geometric Ricci scalar (bottom) are shown versus r_+ for $n = 4$, $\Lambda = -1$, $Q = 1$, $\beta = 1$, and $\alpha = 0.001$ (solid line), $\alpha = 0.1$ (bold line), and $\alpha = 1$ (dashed line).

$$\mathcal{H} = {}_2F_1\left(\frac{1}{2}, \frac{n-2}{2n-2}; \frac{3n-4}{2n-2}; (1-\Gamma^2)\right), \qquad (22)$$

in which ${}_pF_q(a,b;c;d)$ is the hypergeometric function. Since the inclusion of the mentioned NLED models in the Lagrangian of third-order Lovelock gravity with two free parameters α_2 and α_3 makes calculations considerably more complicated, we use a subclass of Lovelock gravity with a relation between the various Lovelock coefficients. In other words, in our model one can choose a special case in which α_3 is a function of α_2 to simplify the complicated TOL field equation and its solutions. Thus, the metric function for TOL gravity may be obtained as [17]

$$f_{\mathrm{TOL}}(r) = 1 + \frac{r^2}{\alpha}[1 - \Psi_{\mathrm{TOL}}^{1/3}], \qquad (23)$$

where

$$\Psi_{\mathrm{TOL}} = 1 + \frac{3\alpha m}{r^n} + \frac{6\alpha\Lambda}{n(n-1)} + \frac{3\alpha\beta^2\Upsilon_n}{n(n-1)}, \qquad (24)$$

and $N(r) = C$ for all the mentioned branches of Lovelock gravity. Hereafter, we choose $N(r) = C = 1$ without loss of generality. In the above equations, we have set $\alpha_2 = \frac{\alpha}{(n-2)(n-3)}$ and $\alpha_3 = \frac{\alpha^2}{3(n-2)(n-3)(n-4)(n-5)}$ for further simplification. It has been shown that these solutions may be interpreted as black-hole solutions with various horizon properties depending on the values of the nonlinearity parameter β (see Refs. [15,18] for more details). Using the series expansion for large distances ($r \gg 1$), one can show that these solutions are asymptotically AdS (with an effective cosmological constant). Besides, we should note that in general there are no restrictions on the Lovelock coefficient α. Although there are a limited number of published papers covering Lovelock gravity (one of which considered negative values for the Lovelock coefficient [23]), in this paper we restrict ourselves to positive α. In addition, in order to obtain physical solutions with real asymptotical behavior, we should regard $\alpha \leq -n(n-1)/(8\Lambda)$ for negative Λ. Since the geometric properties of the solutions were discussed before [15–17,19], in this paper we focus on the thermodynamic stability conditions using the GTD method.

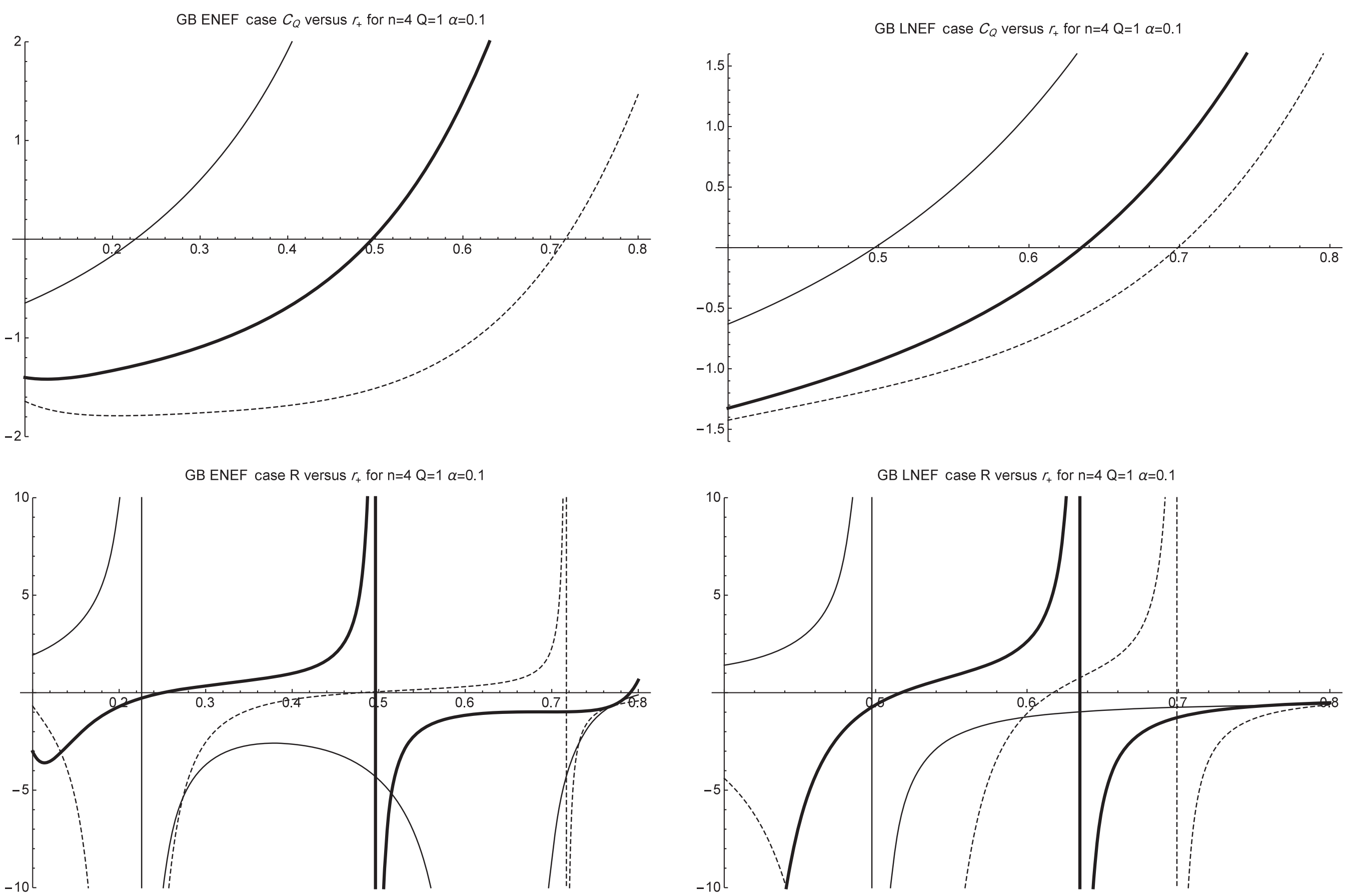

FIG. 5. GB case: ENEF (left) and LNEF (right) branches. The heat capacity (top) and geometric Ricci scalar (bottom) are shown versus r_+ for $n = 4$, $\Lambda = -1$, $Q = 1$, $\alpha = 0.1$, and $\beta = 0.5$ (solid line), $\beta = 1$ (bold line), and $\beta = 2$ (dashed line).

III. THERMODYNAMIC STABILITY

A. Thermodynamic properties

Taking into account third-order Lovelock gravity, it has been shown that the entropy of the asymptotically flat solutions can be written as the Wald formula [24],

$$S = \frac{1}{4}\int d^{n-1}x\sqrt{\tilde{g}}(1 + 2\alpha_2\tilde{R} + 3\alpha_3\tilde{\mathcal{L}}_2), \qquad (25)$$

where $\tilde{g}$ is the determinant of the induced metric $\tilde{g}_{\mu\nu}$, and $\tilde{R}$ and $\tilde{\mathcal{L}}_2$ are, respectively, the Ricci scalar and the Lagrangian of GB gravity for the metric $\tilde{g}_{ab}$ on the $(n-1)$-dimensional spacelike hypersurface. Calculations show that for our black-hole solutions the entropy may be simplified as [16,17,19]

$$S = \frac{V_{n-1}r_+^{n-1}}{4}\begin{cases} 1, & \text{(Einstein)} \\ 1 + \frac{2(n-1)\alpha}{(n-3)r_+^2}, & \text{(GB)} \\ 1 + \frac{2(n-1)}{(n-3)}\frac{\alpha}{r_+^2} + \frac{(n-1)}{(n-5)}\frac{\alpha^2}{r_+^4}, & \text{(TOL)} \end{cases} \qquad (26)$$

where for $\alpha \longrightarrow 0$ the area law is recovered, as is expected. In Eq. (26), r_+ is the event-horizon radius of the black-hole solutions. It is notable that one can obtain Eq. (26) from the Gibbs-Duhem relation [25].

Now, we calculate the flux of the electric field at infinity to obtain the electric charge of the black holes. For the mentioned BI-type NLED theories, we find [16,17,19]

$$Q = \frac{V_{n-1}}{4\pi}q, \qquad (27)$$

which is the same as that in the linear Maxwell theory. Regarding the temporal Killing null generator $\chi = \partial/\partial t$, the electric potential U, measured at infinity with respect to the event horizon, is [26,27]

$$U = A_\mu\chi^\mu|_{r\to\infty} - A_\mu\chi^\mu|_{r=r_+} = \begin{cases} \frac{\beta r_+\sqrt{L_{W_+}}}{2(n-2)(3n-4)}[(n-1)L_{W_+}\zeta_+ + 3n - 4], & \text{(ENEF)} \\ -\frac{2\beta^2 r_+^n}{nq}(\eta_+ - 1), & \text{(LNEF)} \end{cases} \qquad (28)$$

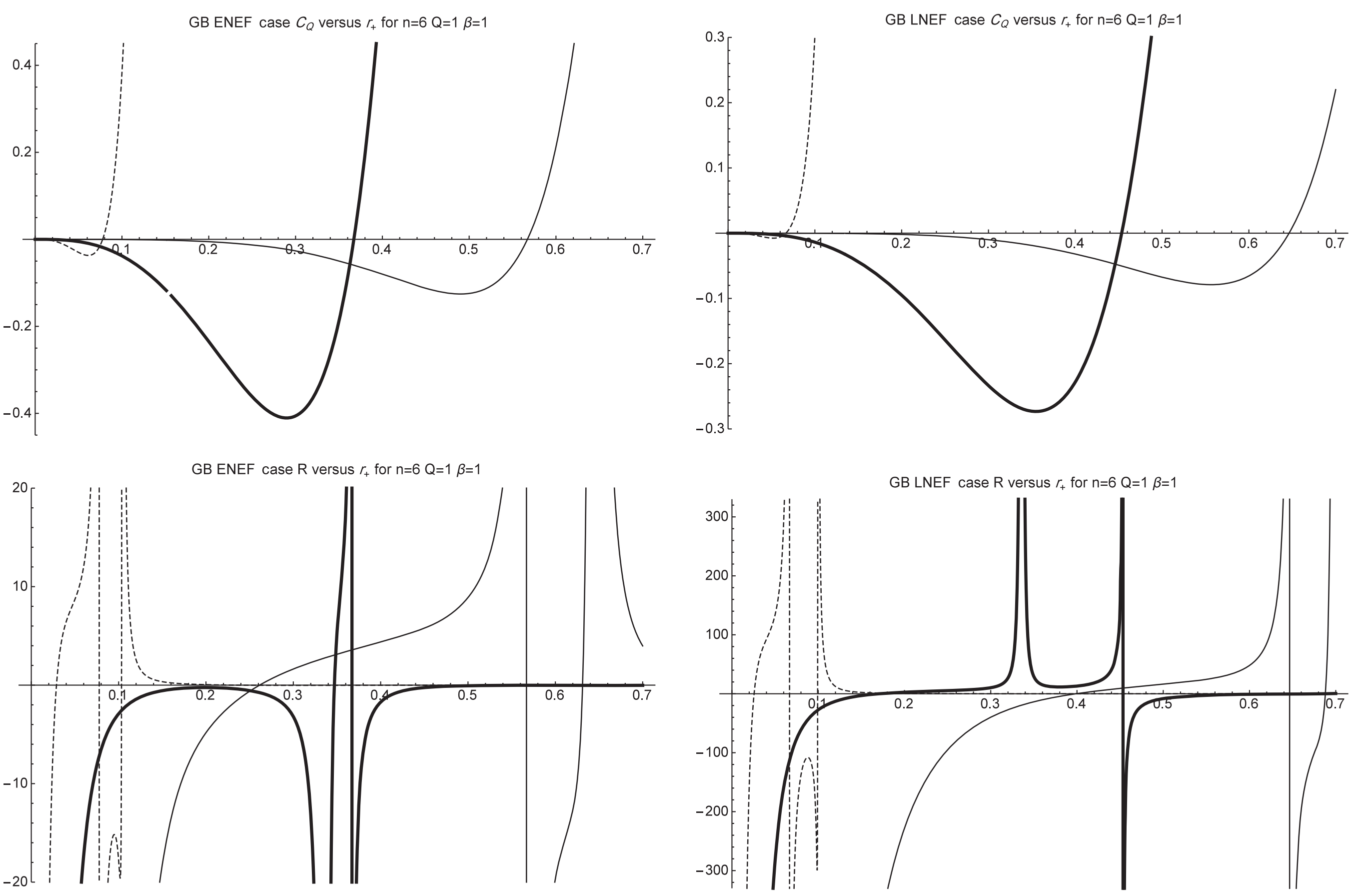

FIG. 6. GB case: ENEF (left) and LNEF (right) branches. The heat capacity (top) and geometric Ricci scalar (bottom) are shown versus r_+ for $n = 6$, $\Lambda = -1$, $Q = 1$, $\beta = 1$, and $\alpha = 0.001$ (solid line), $\alpha = 0.1$ (bold line), and $\alpha = 1$ (dashed line).

where

$$\zeta_+ = {}_1F_1\left(1; \frac{5n-6}{2(n-1)}; \frac{L_{W_+}}{2(n-1)}\right), \tag{29}$$

$$\eta_+ = {}_2F_1\left(-\frac{1}{2}, \frac{-n}{2(n-1)}; \frac{n-2}{2(n-1)}; (1-\Gamma_+^2)\right), \tag{30}$$

and

$$L_{W_+} = \mathrm{Lambert}W\left(\frac{4q^2}{\beta^2 r_+^{2n-2}}\right),$$

$$\Gamma_+ = \sqrt{1 + \frac{q^2}{\beta^2 r_+^{2n-2}}}.$$

In addition, the Hawking temperature of the black hole may be obtained by the use of the surface-gravity interpretation, yielding

$$T_E = \frac{-2\Lambda r_+^2 + (n-1)(n-2) - \frac{\Phi}{r_+}}{4\pi(n-1)r_+}, \tag{31}$$

$$T_{\mathrm{GB}} = \frac{-2\Lambda r_+^4 + (n-1)(n-2)r_+^2 + (n-1)(n-4)\alpha - \Phi r_+}{4\pi r_+(n-1)(r_+^2 + 2\alpha)}, \tag{32}$$

$$T_{\mathrm{TOL}} = \frac{-6\Lambda r_+^6 + 3(n-1)(n-2)r_+^4 + 3(n-1)(n-4)\alpha r_+^2 + (n-1)(n-6)\alpha^2 - 3\Phi r_+^3}{12\pi r_+(n-1)(r_+^2 + \alpha)^2}, \tag{33}$$

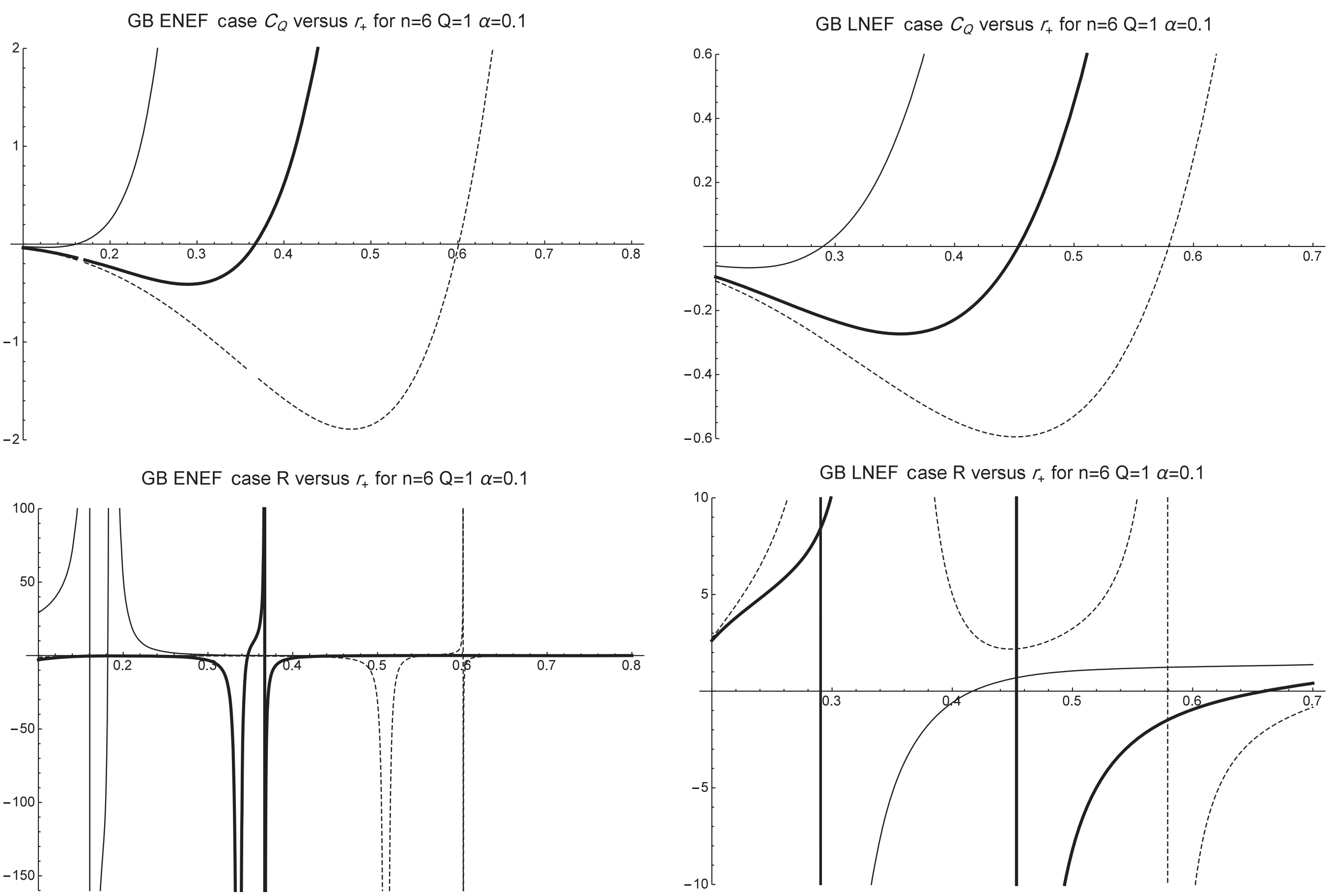

FIG. 7. GB case: ENEF (left) and LNEF (right) branches. The heat capacity (top) and geometric Ricci scalar (bottom) are shown versus r_+ for $n = 6$, $\Lambda = -1$, $Q = 1$, $\alpha = 0.1$, and $\beta = 0.5$ (solid line), $\beta = 1$ (bold line), and $\beta = 2$ (dashed line).

where

$$\Phi = \begin{cases} \beta^2 r_+^3 \left([1 + (\frac{2E}{\beta})^2] e^{\frac{-2E^2}{\beta^2}} - 1 \right), & \text{(ENEF)} \\ 8 r_+^3 \beta^2 \ln \left[1 - (\frac{E}{2\beta})^2 \right] + \frac{4 r_+^3 E^2}{1-(\frac{E}{2\beta})^2}, & \text{(LNEF)} \end{cases}$$

and

$$E = \frac{q}{r_+^{n-1}} \times \begin{cases} \exp\left(-\frac{L_{W_+}}{2}\right), & \text{(ENEF)} \\ \frac{2}{1+\Gamma_+}. & \text{(LNEF)} \end{cases} \tag{34}$$

Following the method of Ref. [15], one can find that there is a critical nonlinearity parameter, β_c, in which the Hawking temperature is positive definite for $\beta < \beta_c$. For $\beta > \beta_c$, there is a minimum value for the horizon radius of physical black holes, r_0, in which T is positive for $r_+ > r_0$.

Regarding the Arnowitt-Deser-Misner approach, we find that the finite mass of a black hole is [28]

$$M = \frac{V_{n-1}}{16\pi} m(n-1), \tag{35}$$

where m can be calculated from $f(r)|_{r=r_+} = 0$ and, therefore, in general the finite mass depends on both the Lovelock coefficients and the nonlinearity parameter.

It has been shown that the obtained conserved and thermodynamic quantities satisfy the first law of thermodynamics [16,17,19],

$$dM = TdS + UdQ. \tag{36}$$

In other words, by combining Eq. (36) with Eqs. (17) [or other metric functions of GB and TOL branches, i.e., Eqs. (19) and (23)], (26), (27), and (35), we find that $(\frac{\partial M}{\partial Q})_S$ and $(\frac{\partial M}{\partial S})_Q$ are the same as those calculated in Eqs. (28) and (31) [or other temperatures of GB and TOL branches, i.e., Eqs. (32) and (33)], respectively.

B. Thermal stability and geometrothermodynamics

Now, we investigate the thermal stability in the canonical ensemble by calculating the heat capacity of the black-hole solutions,

$$C_Q \equiv T \left(\frac{\partial S}{\partial T} \right)_Q = T \left(\frac{\partial^2 M}{\partial S^2} \right)_Q^{-1}. \tag{37}$$

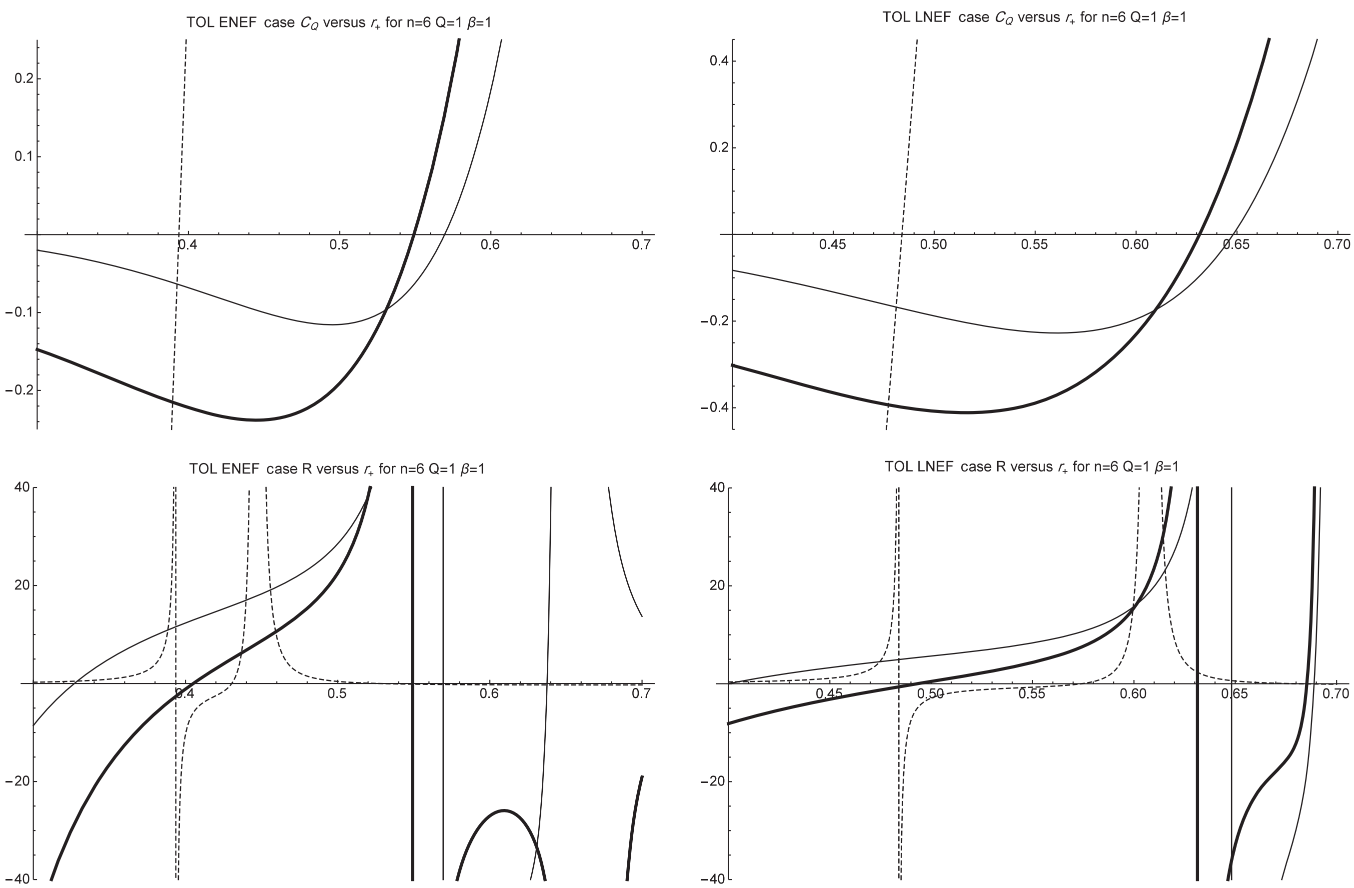

FIG. 8. TOL case: ENEF (left) and LNEF (right) branches. The heat capacity (top) and geometric Ricci scalar (bottom) are shown versus r_+ for $n = 6$, $\Lambda = -1$, $Q = 1$, $\beta = 1$ and $\alpha = 0.001$ (solid line), $\alpha = 0.1$ (bold line) and $\alpha = 1$ (dashed line).

The root of the heat capacity corresponds to the phase transition, and the positivity of C_Q is a sufficient condition for the system to be locally stable [29,30].

Another new method of describing the phase transitions of a thermodynamical systems is the concept of geometry in thermodynamics. In this method one may regard the curvature singularities as the phase transition, and so the curvature can be interpreted as a system interaction. In order to calculate the heat capacity and the curvature singularity using the GTD method, we calculate the finite mass as a function of entropy and electric charge, $M(S, Q)$. One may use Eqs. (26), (31), (32) or (33), and (37) to obtain

$$C_Q = \frac{T}{\left(\frac{\partial^2 M}{\partial S^2}\right)_Q} = \frac{T\left(\frac{\partial S}{\partial r_+}\right)_Q}{\left(\frac{\partial T}{\partial r_+}\right)_Q}.$$

Although an analytical expression for C_Q is too large and thus we cannot evaluate its sign analytically, numerical analysis helps us overcome this problem. In addition, we include Figs. 1–9 to provide additional clarification. Numerical calculations show that there is a lower limit on the horizon radius for the stable AdS solutions. This means that in order to have a stable solution, we should set the horizon radius higher than a lower bound ($r_+ > r_{\mathrm{min}}$) [17]. (We should note that this statement is valid for asymptotically AdS solutions with spherical horizons.)

Now we would like to study the phase transition, which occurs at $r_+ = r_{\mathrm{min}}$. The top panels in Figs. 1–9 show that—regardless of the value of α—r_{min} increases as the nonlinearity parameter β increases.

Considering the effects of higher orders of Lovelock gravity, we find that the behavior of Fig. 4 is different from that in Figs. 6 and 8. By examining these figures, we find that—regardless of the values of q, Λ, and β—the root of the heat capacity does not change for various choices of α in five-dimensional GB gravity. However, for higher-dimensional solutions of GB gravity, an increase of α leads to a decrease of r_{min}. One can check that for independent Lovelock coefficients (α_2 and α_3), the behavior of seven-dimensional TOL gravity is the same as that in five-dimensional GB gravity. Here, we note that this unusual behavior may be expected for five-dimensional GB gravity, seven-dimensional TOL gravity, nine-dimensional fourth-order Lovelock (FOL) gravity, and so on. Considering an $(n+1)$-dimensional spacetime, the contribution of the GB term (TOL term) of Lovelock gravity can be seen for $n \geq 4$ ($n \geq 6$). It has been shown

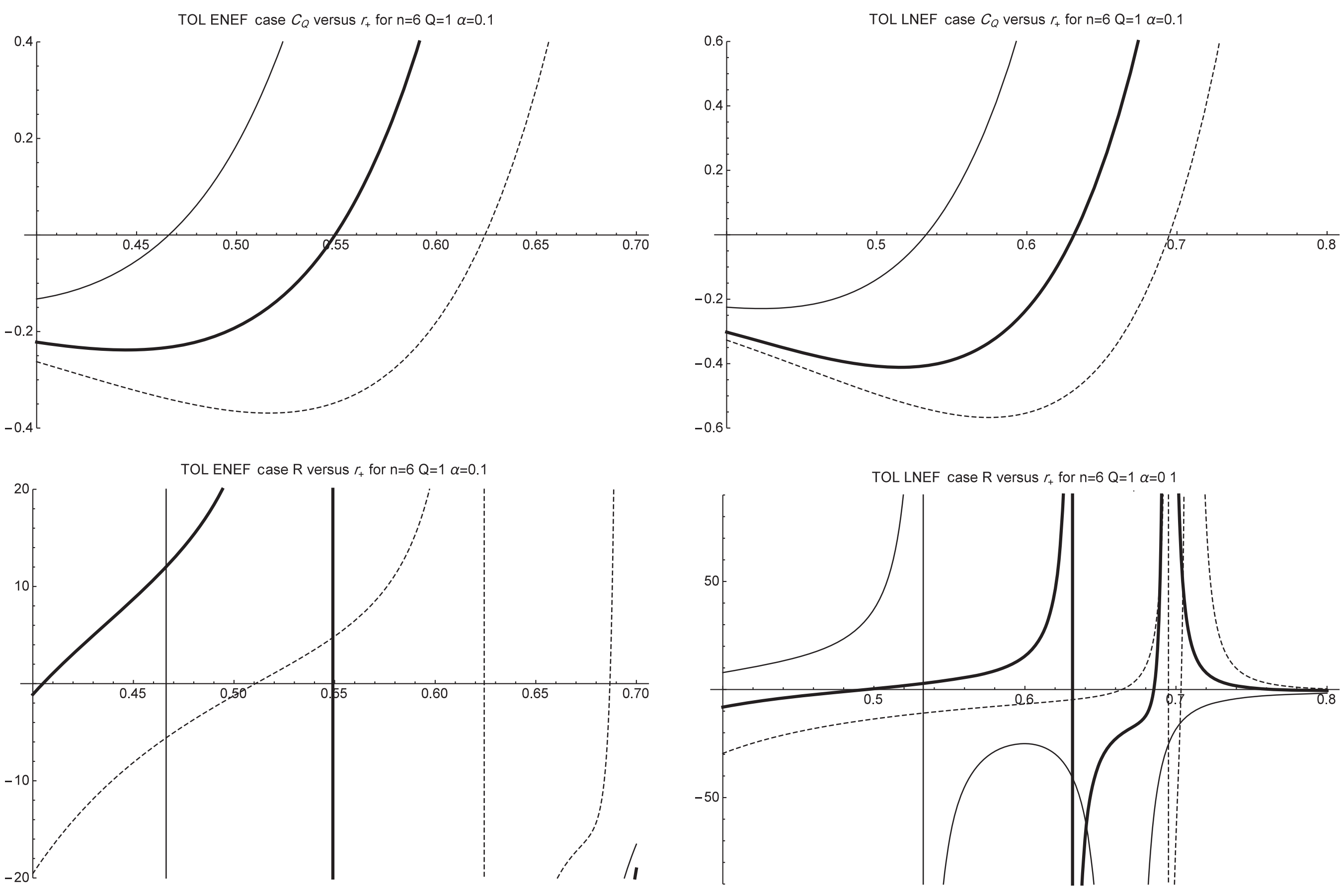

FIG. 9. TOL case: ENEF (left) and LNEF (right) branches. The heat capacity (top) and geometric Ricci scalar (bottom) are shown versus r_+ for $n = 6$, $\Lambda = -1$, $Q = 1$, $\alpha = 0.1$ and $\beta = 0.5$ (solid line), $\beta = 1$ (bold line) and $\beta = 2$ (dashed line).

that the properties of five-dimensional GB solutions are slightly different from higher-dimensional solutions (see Ref. [31] and the geometrical mass interpretation). In addition, one can obtain the same specific behavior for seven-dimensional TOL gravity [32] (by choosing a constant GB parameter α_2 and varying the TOL parameter α_3), nine-dimensional FOL gravity (by choosing constant GB and TOL parameters α_2 and α_3 and varying the FOL parameter α_4), and so on. In other words, it is expected that the GB parameter in five dimensions, the TOL parameter in seven dimensions, and the FOL parameter in nine dimensions have unusual properties, and it may be expected that (unlike higher-dimensional cases) they do not change the location of the vanishing heat capacity. (As we mentioned before, this property is independent of the nonlinearity parameter β, and numerical calculations for $\beta \neq 1$ confirm this point.) In this paper, since we are using a special case in which α_2 is related to α_3, changing α_3 leads to a change in α_2. Therefore, for seven dimensions ($n = 6$), we cannot fix α_2 and vary α_3 to check the effect of α_3, and hence we do not see the unusual behavior of seven-dimensional TOL gravity.

In order to study the phase transition using the GTD approach, we follow the method of Quevedo [1,8–13]. We calculate the Ricci scalar of the Legendre invariant of the Ruppeiner metric and look for its singularities to compare them with the zeros of the heat capacity. Although the Quevedo method is straightforward, analytically calculated results are too large. So, for the sake of brevity we do not write the long equations of the Ricci scalars; instead, we use numerical analysis and some plots to investigate the Ricci scalar's behavior. We plot $R(S, Q)$ as a function of r_+ ($r_+ = r_+(S)$) and compare it with the corresponding heat capacity. Comparing the top and bottom diagrams of Figs. 1–9, we find that the singularities of the Ricci scalar (bottom diagrams) take place at those points where the heat capacity vanishes (top diagrams). Hence, both the GTD method and the usual thermodynamic approach in the canonical ensemble are in agreement with each other, which confirms that the black holes undergo a phase transition.

IV. CONCLUSIONS

In this paper, we considered black-hole solutions of the Einstein, GB, and TOL gravities with two classes of BI-type NLED models. The main goal of this paper was to discuss the phase transition using the GTD method and to compare its consequences with the usual heat capacity in the canonical ensemble. We obtained the thermodynamic quantities and adopted the method of Quevedo to obtain the Ricci scalar of the Legendre invariant of the Ruppeiner metric.

Since the analytical calculations and their corresponding relations were too large, we performed a numerical analysis. Numerical calculations showed that the singularities of the Ricci scalar using the GTD method take place at those points where the heat capacity vanishes in the canonical ensemble. In other words, we (interestingly) found that both the GTD method and the usual thermodynamic stability criterion in the canonical ensemble are in agreement with each other, which confirms that the black holes undergo a phase transition.

Moreover, we studied the effects of the nonlinearity parameter β and the Lovelock coefficient on the location of the critical points. We found that—regardless of the metric parameters—the location of the critical points increases as the nonlinearity parameter β increases. In addition, we showed that although in general increasing the Lovelock coefficient leads to a decrease in the location of the critical points of the phase transition, there are some anomaly cases. We found that this anomaly takes place for five-dimensional GB gravity and may be generalized to seven-dimensional TOL gravity, nine-dimensional FOL gravity, and so on. In other words, the location of the vanishing heat capacity does not change when changing the GB parameter in five dimensions, when changing the TOL parameter in seven dimensions, when changing the FOL parameter in nine dimensions, and so on.

As we mentioned, the asymptotically AdS solutions investigated here (the third-order case) contain only one fundamental constant. An investigation of the third-order case with two independent constants and a generalization of our results to higher orders of Lovelock gravity with one (or more) fundamental constant(s) are interesting subjects for future analysis. Finally, we should note that it is worthwhile to study the phase transition in an extended phase space [33], and this interesting work will appear in a forthcoming publication [34].

ACKNOWLEDGMENTS

We would like to thank the anonymous referee for valuable suggestions. We also acknowledge S. Panahiyan for reading the manuscript. We wish to thank the Shiraz University Research Council. This work has been supported financially by the Research Institute for Astronomy & Astrophysics of Maragha (RIAAM), Iran.

[1] H. Quevedo and A. Sanchez, J. High Energy Phys. 09 (2008) 034.

[2] R. Banerjee, S. K. Modak, and S. Samanta, Phys. Rev. D **84**, 064024 (2011); H. Liu, H. Lu, M. Luo, and K. N. Shao, J. High Energy Phys. 12 (2010) 054; M. Azreg-Ainou, Eur. Phys. J. C **74**, 2930 (2014).

[3] F. Weinhold, J. Chem. Phys. **63**, 2479 (1975).

[4] F. Weinhold, J. Chem. Phys. **63**, 2484 (1975).

[5] G. Ruppeiner, Phys. Rev. A **20**, 1608 (1979).

[6] G. Ruppeiner, Rev. Mod. Phys. **67**, 605 (1995); **68**, 313(E) (1996).

[7] P. Salamon, J. D. Nulton, and E. Ihrig, J. Chem. Phys. **80**, 436 (1984).

[8] H. Quevedo, J. Math. Phys. (N.Y.) **48**, 013506 (2007).

[9] H. Quevedo, Gen. Relativ. Gravit., **40**, 971 (2008).

[10] H. Quevedo, A. Sanchez, S. Taj, and A. Vazquez, Gen. Relativ. Gravit. **43**, 1153 (2011).

[11] A. Bravetti, D. Momeni, R. Myrzakulov, and A. Altaibayeva, Adv. High Energy Phys. **2013**, 549808 (2013).

[12] A. Bravetti, D. Momeni, R. Myrzakulov, and H. Quevedo, Gen. Relativ. Gravit. **45**, 1603 (2013).

[13] H. Quevedo, Gen. Relativ. Gravit. **40**, 971 (2008).

[14] D. Lovelock, J. Math. Phys. (N.Y.) **12**, 498 (1971); N. Deruelle and L. Farina-Busto, Phys. Rev. D **41**, 3696 (1990); G. A. MenaMarugan, Phys. Rev. D **46**, 4320 (1992); **46**, 4340 (1992).

[15] S. H. Hendi, J. High Energy Phys. 03 (2012) 065.

[16] S. H. Hendi, S. Panahiyan, and E. Mahmoudi, Eur. Phys. J. C **74**, 3079 (2014).

[17] S. H. Hendi and A. Dehghani (to be published).

[18] S. H. Hendi, Ann. Phys. (Berlin) **333**, 282 (2013).

[19] S. H. Hendi, Ann. Phys. (Berlin) **346**, 42 (2014).

[20] J. Maldacena, Adv. Theor. Math. Phys. **2**, 231 (1998); E. Witten, Adv. Theor. Math. Phys. **2**, 253 (1998).

[21] H. H. Soleng, Phys. Rev. D **52**, 6178 (1995).

[22] F. Muller-Hoissen, Phys. Lett. **163B**, 106 (1985).

[23] M. H. Dehghani, Phys. Rev. D **70**, 064009 (2004); C. Charmousis, Lect. Notes Phys. **769**, 299 (2009); S. H. Mazharimousavi, M. Halilsoy, and Z. Amirabi, Phys. Lett. A **375**, 3649 (2011); X. H. Ge, B. Wang, S. F. Wu, and G. H. Yang, J. High Energy Phys. 08 (2010) 108.

[24] T. Jacobson and R. C. Myers, Phys. Rev. Lett. **70**, 3684 (1993); R. M. Wald, Phys. Rev. D **48**, R3427 (1993); M. Visser, Phys. Rev. D **48**, 5697 (1993); T. Jacobson, G. Kang, and R. C. Myers, Phys. Rev. D **49**, 6587 (1994); V. Iyer and R. M. Wald, Phys. Rev. D **50**, 846 (1994).

[25] R. B. Mann, Found. Phys. **33**, 65 (2003); M. H. Dehghani, N. Alinejadi, and S. H. Hendi, Phys. Rev. D **77**, 104025 (2008); S. H. Hendi, Eur. Phys. J. C **73**, 2634 (2013).

[26] M. Cvetic and S. S. Gubser, J. High Energy Phys. 04 (1999) 024.

[27] M. M. Caldarelli, G. Cognola, and D. Klemm, Classical Quantum Gravity **17**, 399 (2000).

[28] L. Brewin, Gen. Relativ. Gravit. **39**, 521 (2007).

[29] A. Chamblin, R. Emparan, C. V. Johnson, and R. C. Myers, Phys. Rev. D **60**, 104026 (1999).

[30] P. C. W. Davies, Proc. R. Soc. A **353**, 499 (1977).

[31] M. H. Dehghani, Phys. Rev. D **70**, 064019 (2004).

[32] A. Dehghani, M.Sc. Thesis, Shiraz University, 2014.

[33] D. Kubiznak and R. B. Mann, J. High Energy Phys. 07 (2012) 033; J. X. Mo and W. B. Liu, Eur. Phys. J. C **74**, 2836 (2014); S. H. Hendi and M. H. Vahidinia, Phys. Rev. D **88**, 084045 (2013).

[34] S. H. Hendi, S. Panahiyan, and B. Eslam Panah (to be published).